# Non-Linear Rigid Body Dynamics: Energy and Momentum Conserving Algorithm

**Fernando A. Rochinha**[1], **Rubens Sampaio**[2]

**Abstract:** The dynamics of flexible systems, such as robot manipulators, mechanical chains or cables, is becoming increasingly important in engineering. The main question arising from the numerical modelling of large overall motions of multibody systems is an appropriate treatment for the large rotations. In the present work an alternative approach is proposed leading to a time-stepping numerical algorithm which achieves stable solutions combined with high precision. In particular, in order to check the performance of the proposed approach, two examples having preserved constants of the motion are presented.

**keyword:** rigid body, nonlinear dynamics, conservation

## 1 Introduction

Recently there has been a great interest in the study of nonlinear dynamics of structures and its applications to a wide variety of engineering problems: robotics, spacecraft dynamics and attitude control, vehicle dynamics, and large structures vibration. Indeed, there is a growing literature (see, for example, Borri,Mello and Atluri (1991); Hughes (1986); Vu-Quoc and Simo (1988); Downer, Park and Chiou (1992); Sharf (1996) and references therein).

The present article is concerned with the nonlinear dynamics of rigid bodies. The importance of studying rigid bodies is based in two main points. First, the modelling of multibody systems is often done assuming that some parts of the system are rigid. Second, the experience obtained with rigid bodies might be used in a flexible systems analysis. In particular, the approach to the rotational degrees of freedom plays a crucial role in the modelling and numerical approximation, using finite element method, of rods and shells, which are often used as links in multibody systems, (see Vu-Quoc and Simo (1988); Rochinha (1990) and Le Tallec, Mani and Rochinha (1992)). Thus, in order to better establish and assess the performance of some specific approach, the dynamics of a single rigid body is often used as prototype problem. From a numerical standpoint it represents a significant test due to its high degree of nonlinearity.

The dynamic response associated with the rotational degrees of freedom leads to an evolution problem in the rotation group, which can be parametrized in several different ways [Hughes (1986); Trindade and Sampaio (1999)]. In the present work, a variational formulation, closely related to that proposed by Le Tallec, Mani and Rochinha (1992), based on the use of directors [Antman and Kenney (1981)] is presented. The use of lagrange multipliers avoids some difficulties in obtaining the tangent operators inherent to numerical procedures.

The objective of the present work is to develop a class of numerical algorithms dedicated to the simulation of the nonlinear dynamics of rigid bodies. Temporal or spatial discretizations of the dynamics generated by a Hamiltonian system need not inherit the conservation laws of the continuum system such as energy or momentum conservation. In the literature, numerical schemes capable of preserving those quantities are known as conserving algorithms, see Lewis and Simo(1994). Three main reasons can be pointed out to motivate the construction of such algorithms: the role played by those quantities in the physical and mathematical context; the enhanced numerical capabilities of those algorithms and, finally, the conserved quantities often represent qualitative features of the long term dynamics. The energy conservation, for instance, is accepted as a demonstration of numerical stability in the nonlinear range [Richtmyer and Morton(1967)].

The design of conserving algorithms has attracted a lot of attention in recent years. In the context of dynamics of structures the pioneer work seems to be due to Hughes, Liu and Caughy (1978), that has presented an algorithm relying on the use of Lagrange multipliers in order to assure the energy conservation. More recently, Simo and coworkers (1991,1992,1993,1994,1996) has introduced energy-momentum algorithms in the context of rigid body, elastodynamics and nonlinear rods. In fact, there are an extensive literature: Gonzalez(1996), Bayliss and Isaacson (1975), Zhong and Marsden (1988), La Budde and Greenspan (1976 a,b), Crisfield and Shi(1994), Galvanetto and Crisfield(1996), Bauchau,Damilano and Theron (1995).

## 2 Non-linear Rigid Body Dynamics

In the following, a brief summary of the dynamics of a rigid body is presented. Further details can be found in the standard literature, for instance Whittaker(1944).

[1] Mechanical Engineering Department, EE-COPPE-UFRJ Cx. Postal 68503; 21945-970, Rio de Janeiro, RJ; Brazil

[2] Mechanical Engineering Department– PUC-Rio Rua Marquês de São Vicente, 225; 22453-900, Rio de Janeiro, RJ; Brazil

### 2.1 Kinematics

Let $\boldsymbol{B} \in \boldsymbol{R}^3$ be the reference placement of a solid body, with particles labeled by $\mathbf{X}$. So, the motion of the body is described by the mapping:

$$\begin{aligned} \phi:\ \boldsymbol{B}\times[0,T] &\rightarrow \boldsymbol{R}^3 \\ (\mathbf{X},t) &\rightarrow \mathbf{x} \end{aligned} \tag{1}$$

where $t$ denotes the time, $T$ represents the total time of observation and $\boldsymbol{R}^3$ is the ordinary 3D-Euclidian space. Throughout this paper, bold letters are used to designate vectors.

As in a rigid body the distance between any two points must remain the same during the motion, the position of each particle can be put in the following form:

$$\mathbf{x}(t) = \mathbf{r}(t) + \sum_{i=1}^{3} X_i\, \mathbf{d_i}(t) \tag{2}$$

where $\mathbf{r}$ defines the position of the center of mass and $\mathbf{d_i}$ are vector fields called directors [see Antman and Kenney (1981)], forming at each instant $t$ an orthonormal basis attached to the body. Within the rigid body literature, the basis $\{\mathbf{d_i}\}$ is known as the body frame.

In Eq. 2, $\mathbf{r}$ takes into account the translation of the body and its rotation is described by the comparison between the directors and a fixed (inertial) basis. Thus, the configuration of the body is represented by the pair

$$(\mathbf{r}, \mathbf{d_i}) \ \in \ \boldsymbol{R}^3 \text{ x } K \tag{3}$$

with the nonlinear manifold K defined by

$$K = \{(\mathbf{g_1}, \mathbf{g_2}, \mathbf{g_3}) \in \boldsymbol{R}^9 \ / \ \ \mathbf{g_i}\cdot\mathbf{g_j} = \delta_{ij}\, i,j = 1,2,3\}$$

where $\delta_{ij}$ represents the delta of Kronecker. Consequently, one refers to $\boldsymbol{R}^3$ x $K$ as the abstract configuration manifold of the rigid body.

**Remark:** Indeed, $K$ and the special group of rotations $SO(3)$, Lewis and Simo (1994), can be identified by the isomorphism:

$$\mathbf{d_i} = \mathbf{Q}\,\mathbf{D_i} \quad (i = 1,2,3) \tag{4}$$

where $\mathbf{Q}$ is a rotation belonging to $SO(3)$ and $\mathbf{D_i}$ are the directors in the reference placement ($t = 0$), which, without loss of generality, can be taken coincident with the principal directions of inertia. So, the rotation can be recast as $\mathbf{Q} = \sum_{i=1}^{3} \mathbf{d_i} \otimes \mathbf{D_i}$, where $\otimes$ represents the tensorial product.

The velocities and accelerations fields in the present theory are

- Translational Motion: $\mathbf{v} = \dot{\mathbf{r}}$ ; $\mathbf{a} = \dot{\mathbf{v}}$
- Rotational Motion: $\dot{\mathbf{d}}_\mathbf{i}$ ; $\ddot{\mathbf{d}}_\mathbf{i}$

where $\dot{(\ )}$ stands for the time derivative of $(\ )$. The first two fields are the translational velocity and the translational acceleration. The others describe the velocity and acceleration of the angular motion and are related to the angular velocity $\mathbf{w}$ and the angular acceleration $\boldsymbol{\alpha}$ of the body by means of:

$$\dot{\mathbf{d}}_\mathbf{i} = \mathbf{w} \wedge \mathbf{d_i} \tag{5}$$

$$\ddot{\mathbf{d}}_\mathbf{i} = \boldsymbol{\alpha} \wedge \mathbf{d_i} + \mathbf{w} \wedge \dot{\mathbf{d}}_\mathbf{i} \tag{6}$$

where $\wedge$ denotes the ordinary vector product.

As was mentioned in the introduction, the linear and angular momenta, which are given, respectively, by $\mathbf{L} = \int_{\boldsymbol{B}} \rho\, \dot{\phi}\, \mathbf{dX}$ and $\mathbf{J} = \int_{\boldsymbol{B}} \rho\, \phi \wedge \dot{\phi}\, \mathbf{dX}$, where $\rho$ is the mass density, play a crucial role in the understanding of the dynamics of a rigid body. Using Eq. 2 in the above expressions, the linear and angular momenta, in the present context,are given respectively by

$$\mathbf{L} = M\mathbf{v} \tag{7}$$

where $M$ is the total mass given by $\int_{\boldsymbol{B}} \rho\, d\mathbf{X}$ and

$$\begin{aligned} \mathbf{J} = \mathbf{L} &+ \frac{I_{33} - I_{11} + I_{22}}{2}\mathbf{d_1} \wedge \dot{\mathbf{d}}_\mathbf{1} + \\ &\frac{I_{11} - I_{22} + I_{33}}{2}\mathbf{d_2} \wedge \dot{\mathbf{d}}_\mathbf{2} + \frac{I_{22} - I_{33} + I_{11}}{2}\mathbf{d_3} \wedge \dot{\mathbf{d}}_\mathbf{3} - \\ &I_{12}(\mathbf{d_1} \wedge \dot{\mathbf{d}}_\mathbf{2} + \mathbf{d_2} \wedge \dot{\mathbf{d}}_\mathbf{1}) - I_{13}(\mathbf{d_1} \wedge \dot{\mathbf{d}}_\mathbf{2} + \mathbf{d_1} \wedge \dot{\mathbf{d}}_\mathbf{2}) - \\ &I_{23}(\mathbf{d_1} \wedge \dot{\mathbf{d}}_\mathbf{2} + \mathbf{d_1} \wedge \dot{\mathbf{d}}_\mathbf{2}) \end{aligned} \tag{8}$$

where the scalars $I_{ij} = I_{ji}$ are the components of the moment of inertia tensor

$$\mathbf{I} = \sum_{i=1}^{3}\sum_{j=1}^{3} I_{ij}(\mathbf{d_i} \otimes \mathbf{d_j})$$

defined by

$$I_{ij} = \begin{cases} \int_{\boldsymbol{B}} \rho(||\mathbf{X}||^2 - X_i^2)\mathbf{dX} & \text{if i=j} \\ \int_{\boldsymbol{B}} \rho X_i X_j \mathbf{dX} & \text{otherwise} \end{cases}$$

**Remark**. Using Eq. 5 and the relations $\mathbf{d_i} \wedge \dot{\mathbf{d}}_\mathbf{i} = \mathbf{w} - (\mathbf{w}\cdot\mathbf{d_i})\ \mathbf{d_i}$ and $\mathbf{d_i} \wedge \dot{\mathbf{d}}_\mathbf{j} = -(\mathbf{w}\cdot\mathbf{d_i})\ \mathbf{d_j}$, the above expression for the angular momentum can be put in the classical form of the rigid body dynamics

$$\mathbf{J} = \mathbf{L} + \boldsymbol{\pi}$$

where $\boldsymbol{\pi} = \mathbf{Iw}$ is the spatial angular momentum relative to the center of mass.

### 2.2 Equations of Motion: Variational Formulation

In the present work, the equations of motion, balance of linear and angular momentum of a rigid body will be presented in a variational form based on the Hamilton's Principle version presented by Bayley(1997). This version differs from the classical least action variational principle by the inclusion of an

end-point term, e.g

$$\int_{t1}^{t2} \delta \boldsymbol{L}\ dt - \frac{\partial T}{\partial \dot{\mathbf{r}}}\mathbf{p}|_{t1}^{t2} - \sum_{i=1}^{3} \frac{\partial T}{\partial \dot{\mathbf{d}}_\mathbf{i}}\mathbf{g_i}|_{t1}^{t2} = \mathbf{0} \tag{9}$$

where $[t_1, t_2] \subset [0, T]$, the lagrangian $\boldsymbol{L} = T - V$, in which $T$ and $V$ are, respectively, the kinetic and potential energy and the vector fields $\mathbf{p}$ and $\mathbf{g_i}$ will be introduced next. The notation $f|_{t1}^{t2} = f(t1) - f(t2)$ is used to represent the end–point terms. The equivalence between of the variational formulation presented below and the classical Euler's equation for the rigid body is presented in the Appendix A.

Based on the general formula of the kinetic energy of a continuum, an expression for the kinetic energy in the present modelling of rigid body is obtained using Eq. 2

$$\begin{aligned} T = \int_{\boldsymbol{B}} \frac{1}{2}\ \rho\ \dot{\mathbf{x}} \cdot \dot{\mathbf{x}}\ dS = \frac{1}{2}\{\int_{\boldsymbol{B}} \rho(\mathbf{v} + \sum_{i=1}^{3} X_i\ \dot{\mathbf{d}}_\mathbf{i})^2 dS\} = \\ \frac{1}{2}\{\int_{\boldsymbol{B}} \rho \mathbf{v} \cdot \mathbf{v} dS + \int_{\boldsymbol{B}} \rho \sum_{i=1}^{3} X_i^2 \dot{\mathbf{d}}_\mathbf{i} \cdot \dot{\mathbf{d}}_\mathbf{i} dS + \\ \int_{\boldsymbol{B}} \rho \sum_{i=1}^{3}\sum_{j=1}^{3} X_i X_j \dot{\mathbf{d}}_\mathbf{i} \cdot \dot{\mathbf{d}}_\mathbf{j} dS\} \end{aligned} \tag{10}$$

Using the definitions of inertia components introduced before, the expression above is rephrased yielding

$$\begin{aligned} T = \frac{1}{2} M \mathbf{v} \cdot \mathbf{v} + \frac{1}{2}\{\{\frac{I_{33} - I_{11} + I_{22}}{2}\}\dot{\mathbf{d}}_\mathbf{1} \cdot \dot{\mathbf{d}}_\mathbf{1} + \\ \{\frac{I_{11} - I_{22} + I_{33}}{2}\}\dot{\mathbf{d}}_\mathbf{2} \cdot \dot{\mathbf{d}}_\mathbf{2} + \{\frac{I_{22} - I_{33} + I_{11}}{2}\}\dot{\mathbf{d}}_\mathbf{3} \cdot \dot{\mathbf{d}}_\mathbf{3} - \\ 2\ I_{12}\dot{\mathbf{d}}_\mathbf{1} \cdot \dot{\mathbf{d}}_\mathbf{2} - 2\ I_{13}\dot{\mathbf{d}}_\mathbf{1} \cdot \dot{\mathbf{d}}_\mathbf{3} - 2\ I_{23}\dot{\mathbf{d}}_\mathbf{2} \cdot \dot{\mathbf{d}}_\mathbf{3}\} \end{aligned} \tag{11}$$

The potential energy associated to the external loads is given by

$$V = -\mathbf{f} \cdot \mathbf{r} - \mathbf{f_1} \cdot \mathbf{d_1} - \mathbf{f_2} \cdot \mathbf{d_2} - \mathbf{f_3} \cdot \mathbf{d_3} \tag{12}$$

where the $\mathbf{f_i}$ ($\mathbf{i}$=1,3) are implicitly defined by

$$\mathbf{m} = \mathbf{d_1} \wedge \mathbf{f_1} + \mathbf{d_2} \wedge \mathbf{f_2} + \mathbf{d_3} \wedge \mathbf{f_3} \tag{13}$$

and $\mathbf{m}$ and $\mathbf{f}$ are the total torque and the resultant force applied in the center of mass.

So, from the Lagrangian $\boldsymbol{L} = T - V$ defined over $\boldsymbol{R}^3$ x $K$, the following variational formulation based on Eq. 9 is introduced

$$\begin{aligned} \int_{t1}^{t2} \{m\mathbf{v} \cdot \dot{\mathbf{p}} + \mathbf{f} \cdot \mathbf{p}\}\ dt\ - m\mathbf{v} \cdot \mathbf{p}|_{t1}^{t2} + \\ \int_{t1}^{t2} \{(\frac{I_{33} - I_{11} + I_{22}}{2})\ \dot{\mathbf{d}}_\mathbf{1} \cdot \dot{\mathbf{g}}_\mathbf{1} + (\frac{I_{11} - I_{22} + I_{33}}{2})\ \dot{\mathbf{d}}_\mathbf{2} \cdot \dot{\mathbf{g}}_\mathbf{2} + \\ (\frac{I_{22} - I_{33} + I_{11}}{2})\ \dot{\mathbf{d}}_\mathbf{3} \cdot \dot{\mathbf{g}}_\mathbf{3} - I_{12}\ \dot{\mathbf{d}}_\mathbf{2} \cdot \dot{\mathbf{g}}_\mathbf{1} - I_{12}\ \dot{\mathbf{d}}_\mathbf{1} \cdot \dot{\mathbf{g}}_\mathbf{2} - \\ I_{13}\ \dot{\mathbf{d}}_\mathbf{3} \cdot \dot{\mathbf{g}}_\mathbf{1} - I_{13}\ \dot{\mathbf{d}}_\mathbf{1} \cdot \dot{\mathbf{g}}_\mathbf{3} - I_{23}\ \dot{\mathbf{g}}_\mathbf{2} \cdot \dot{\mathbf{d}}_\mathbf{3} - I_{23}\ \dot{\mathbf{d}}_\mathbf{2} \cdot \dot{\mathbf{g}}_\mathbf{3}\}\ dt \\ - \{\{(\frac{I_{33} - I_{11} + I_{22}}{2})\ \dot{\mathbf{d}}_\mathbf{1} \cdot \mathbf{g}_\mathbf{1} + (\frac{I_{11} - I_{22} + I_{33}}{2})\ \dot{\mathbf{d}}_\mathbf{2} \cdot \mathbf{g}_\mathbf{2} + \\ (\frac{I_{22} - I_{33} + I_{11}}{2})\ \dot{\mathbf{d}}_\mathbf{3} \cdot \mathbf{g}_\mathbf{3} - I_{12}\ \dot{\mathbf{d}}_\mathbf{2} \cdot \mathbf{g}_\mathbf{1} - I_{12}\ \dot{\mathbf{d}}_\mathbf{1} \cdot \mathbf{g}_\mathbf{2} - \\ I_{13}\ \dot{\mathbf{d}}_\mathbf{3} \cdot \mathbf{g}_\mathbf{1} - I_{13}\ \dot{\mathbf{d}}_\mathbf{1} \cdot \mathbf{g}_\mathbf{3} - I_{23}\ \mathbf{g}_\mathbf{2} \cdot \mathbf{d}_\mathbf{3} - I_{23}\ \dot{\mathbf{d}}_\mathbf{2} \cdot \mathbf{g}_\mathbf{3}\}|_{t1}^{t2} \\ + \int_{t1}^{t2} \{\mathbf{f_1} \cdot \mathbf{g_1} + \mathbf{f_2} \cdot \mathbf{g_2} + \mathbf{f_3} \cdot \mathbf{g_3}\}\ = 0 \\ \forall (\mathbf{p}, \mathbf{g_i}) \in R^3 \text{ x } dK \end{aligned} \tag{14}$$

where dK is the tangent space to K given by

$$dK = \{(\mathbf{g_1}, \mathbf{g_2}, \mathbf{g_3}) \in R^9;\ \mathbf{g}_i = \mathbf{U} \wedge \mathbf{d}_i;\ \mathbf{U} \in R^3\}$$

For numerical purposes, the form of Eq. 14 is rephrased by using lagrange multipliers, yielding

$$\begin{aligned} \int_{t1}^{t2} \{m\mathbf{v} \cdot \dot{\mathbf{p}} + \mathbf{f} \cdot \mathbf{p}\}\ dt\ - m\mathbf{v} \cdot \mathbf{p}|_{t1}^{t2} + \\ \int_{t1}^{t2} \{(\frac{I_{33} - I_{11} + I_{22}}{2})\ \dot{\mathbf{d}}_\mathbf{1} \cdot \dot{\mathbf{g}}_\mathbf{1} + (\frac{I_{11} - I_{22} + I_{33}}{2})\ \dot{\mathbf{d}}_\mathbf{2} \cdot \dot{\mathbf{g}}_\mathbf{2} + \\ (\frac{I_{22} - I_{33} + I_{11}}{2})\ \dot{\mathbf{d}}_\mathbf{3} \cdot \dot{\mathbf{g}}_\mathbf{3} - I_{12}\ \dot{\mathbf{d}}_\mathbf{2} \cdot \dot{\mathbf{g}}_\mathbf{1} - I_{12}\ \dot{\mathbf{d}}_\mathbf{1} \cdot \dot{\mathbf{g}}_\mathbf{2} - \\ I_{13}\ \dot{\mathbf{d}}_\mathbf{3} \cdot \dot{\mathbf{g}}_\mathbf{1} - I_{13}\ \dot{\mathbf{d}}_\mathbf{1} \cdot \dot{\mathbf{g}}_\mathbf{3} - I_{23}\ \dot{\mathbf{g}}_\mathbf{2} \cdot \dot{\mathbf{d}}_\mathbf{3} - I_{23}\ \dot{\mathbf{d}}_\mathbf{2} \cdot \dot{\mathbf{g}}_\mathbf{3}\}\ dt \\ - \{\{(\frac{I_{33} - I_{11} + I_{22}}{2})\ \dot{\mathbf{d}}_\mathbf{1} \cdot \mathbf{g}_\mathbf{1} + (\frac{I_{11} - I_{22} + I_{33}}{2})\ \dot{\mathbf{d}}_\mathbf{2} \cdot \mathbf{g}_\mathbf{2} + \\ (\frac{I_{22} - I_{33} + I_{11}}{2})\ \dot{\mathbf{d}}_\mathbf{3} \cdot \mathbf{g}_\mathbf{3} - I_{12}\ \dot{\mathbf{d}}_\mathbf{2} \cdot \mathbf{g}_\mathbf{1} - I_{12}\ \dot{\mathbf{d}}_\mathbf{1} \cdot \mathbf{g}_\mathbf{2} - \\ I_{13}\ \dot{\mathbf{d}}_\mathbf{3} \cdot \mathbf{g}_\mathbf{1} - I_{13}\ \dot{\mathbf{d}}_\mathbf{1} \cdot \mathbf{g}_\mathbf{3} - I_{23}\ \mathbf{g}_\mathbf{2} \cdot \mathbf{d}_\mathbf{3} - I_{23}\ \dot{\mathbf{d}}_\mathbf{2} \cdot \mathbf{g}_\mathbf{3}\}|_{t1}^{t2} - \\ \int_{t1}^{t2} \sum_{i=1}^{3}\sum_{j=1}^{3} \lambda_{ij}\{\mathbf{d_i} \cdot \mathbf{g_j} + \mathbf{d_j} \cdot \mathbf{g_i}\}\ dt + \int_{t1}^{t2} \sum_{i=1}^{3} \mathbf{f_i} \cdot \mathbf{g_i} dt = 0 \\ \forall (\mathbf{p}, \mathbf{g_i}) \in R^3 \text{ x } R^9 \end{aligned} \tag{15}$$

where $\lambda_{ij} = \lambda_{ji}$ are the lagrange multipliers associated with the orthonormality of the directors and, consequently, to the rigid body condition.

## 3 Energy-Momentum Conserving Algorithm

The numerical algorithm that will be introduced in the present chapter is based on a discrete version of the variational equation Eq. 16. The numerical scheme is designed in order to preserve exactly the conservation laws underlying the dynamics of the time-continuum problem, namely the conservation of linear and angular momenta and energy.

### *3.1 Discrete Varitional Equation*

In the numerical context, the variational formulation is substituted by a discrete version. For this purpose let $[t_n, t_{n+1}] \subset [0, T]$ be a typical interval where: $[0, T] = \cup_{n=0}^{N}[t_n, t_{n+1}]$ and $\Delta t_n = t_{n+1} - t_n$ be the time step. Thus, the following discrete form is introduced

$$\begin{aligned} \rho(\mathbf{v}_{n+1} - \mathbf{v}_n) \cdot \mathbf{p} + I_1\{\dot{\mathbf{d}}_{\mathbf{1}n+1} \cdot \mathbf{g}_{\mathbf{1}n+1} - \dot{\mathbf{d}}_{\mathbf{1}n} \cdot \mathbf{g}_{\mathbf{1}n}\} + \\ I_2\{\dot{\mathbf{d}}_{\mathbf{2}n+1} \cdot \mathbf{g}_{\mathbf{2}n+1} - \dot{\mathbf{d}}_{\mathbf{2}n} \cdot \mathbf{g}_{\mathbf{2}n}\} \\ + I_3\{\dot{\mathbf{d}}_{\mathbf{3}n+1} \cdot \mathbf{g}_{\mathbf{3}n+1} - \dot{\mathbf{d}}_{\mathbf{3}n} \cdot \mathbf{g}_{\mathbf{3}n}\} \end{aligned}$$

$$+\frac{1}{2}\Delta t\{\sum_{i,j=1}^{3}\lambda_{ij}{}_{n+\frac{1}{2}}\{\{\mathbf{d}_{\mathbf{i}n+1}\cdot\mathbf{g}_{\mathbf{j}n+1}+\mathbf{d}_{\mathbf{j}n+1}\cdot\mathbf{g}_{\mathbf{i}n+1}\}+$$

$$\{\mathbf{d}_{\mathbf{i}n}\cdot\mathbf{g}_{\mathbf{j}n}+\mathbf{d}_{\mathbf{j}n}\cdot\mathbf{g}_{\mathbf{i}n}\}\}\}=\Delta t\{\mathbf{f}_{n+\frac{1}{2}}\cdot\mathbf{p}-\sum_{i=1}^{3}\mathbf{f}_{\mathbf{i}n+\frac{1}{2}}\cdot\mathbf{g}_{\mathbf{i}n+\frac{1}{2}}\} \quad (16)$$

where $I_1=\frac{I_{33}-I_{11}+I_{22}}{2}$, $I_2=\frac{I_{11}-I_{22}+I_{33}}{2}$ and $I_3=\frac{I_{22}-I_{33}+I_{11}}{2}$ and $\{\}_n$ stands for the numerical approximation of $\{\}$ in the instant $n$. In particular the subscript $n+\frac{1}{2}$ represents the average between the values of the function in times $t_n$ and $t_{n+1}$. In the above expression, the directors are taken coincident with the principal directions of inertia, what does not represent any loss of generality.

The discrete form Eq. 16 is supplemented by the following update formulae for the configuration and velocity field

- translational component

$$\mathbf{r}_{n+1}=\mathbf{r}_n+\Delta t\,\mathbf{v}_{n+\frac{1}{2}} \quad (17)$$

- rotational component

$$\mathbf{d}_{\mathbf{i}n+1}=\mathbf{Q}_n^{n+1}\mathbf{d}_{\mathbf{i}n} \quad (18)$$

where $\mathbf{Q}_n^{n+1}\in SO(3)$ is the orthogonal transformation between the initial and final configurations, which can be described, for instance, by the exponential map, Whittaker(1944), or the cay transform, Lewis and Simo(1994). Both options, which are mappings between $R^3$ and SO(3), are explored in the present work. An important fact for numerical purposes is that for $SO(3)$ the exponential map has a closed-form expression given by the classical formula of Euler and Rodrigues, see Whittaker(1944):

$$\mathbf{Q}_n^{n+1}=\exp[\theta]=\mathbf{1}+\frac{\sin||\theta||}{||\theta||}\,\hat{\theta}+\frac{1}{2}\frac{\sin^2[\frac{1}{2}||\theta||]}{[\frac{1}{2}||\theta||]^2}\hat{\theta}^2 \quad (19)$$

where $\theta$ represents the rotation vector, with rotation angle $||\theta||$. Besides, $\mathbf{1}$ is the identity operator and $\hat{\theta}$ is the skew-symmetric matrix related to the rotation vector by the relation: $\hat{\theta}h=\theta\wedge h$, for $h$ any vector of $R^3$. Indeed, the exponential map can be parametrized in several ways, see Hughes(1986), Borri, Mello and Atluri(1991), Géradin and Rixen(1995), Trindade and Sampaio(1999), for instance, but the use of quaternions is now well established as an optimal singularity free parametrization.

As in the case of the exponential map, the cay transform has also a closed form given by

$$\mathbf{Q}_n^{n+1}=cay[\theta]=[\mathbf{1}-\frac{\hat{\theta}}{2}]^{-1}[\mathbf{1}+\frac{\hat{\theta}}{2}] \quad (20)$$

which, with aid of the Neumann series for the computation of the inverse matrix, results in

$$\mathbf{Q}_n^{n+1}=cay[\theta]=\mathbf{1}+\frac{2}{1+\frac{1}{2}||\theta||^2}[\frac{1}{2}\hat{\theta}+\frac{1}{4}\hat{\theta}^2] \quad (21)$$

Each one of the possibilities, exponential map or cay transform, leads to a different formulae for the update of the rotational fields. Starting from the exponential map, the following mid-point approximation for the director velocity is proposed

$$\frac{\mathbf{d}_{\mathbf{i}n+1}-\mathbf{d}_{\mathbf{i}n}}{\Delta t}=\frac{\dot{\mathbf{d}}_{\mathbf{i}n+1}+\mathbf{Q}_n^{n+1}\dot{\mathbf{d}}_{\mathbf{i}n}}{2}$$

leading to

$$\dot{\mathbf{d}}_{\mathbf{i}n+1}=2\frac{\mathbf{d}_{\mathbf{i}n+1}-\mathbf{d}_{\mathbf{i}n}}{\Delta t}-\mathbf{Q}_n^{n+1}\dot{\mathbf{d}}_{\mathbf{i}n}$$

Unfortunately, the above formulae does not inherit the velocity constraint $\dot{\mathbf{d}}_{\mathbf{i}n+1}\cdot\mathbf{d}_{\mathbf{i}n+1}=0$, which is a direct consequence of Eq. 5. By the way, the exponential map can be recast as

$$\exp[\theta]=\mathbf{1}+\hat{\theta}+\frac{\hat{\theta}^2}{2}+\frac{\hat{\theta}^3}{3!}+\cdots$$

Thus, retaining the linear terms of the series, the update velocity formulae is approximated by

$$\dot{\mathbf{d}}_{\mathbf{i}n+1}=\frac{2}{\Delta t}\hat{\theta}\mathbf{d}_{\mathbf{i}n+1}-\mathbf{Q}_n^{n+1}\dot{\mathbf{d}}_{\mathbf{i}n} \quad (22)$$

which will guarantee that the updated velocity satisfies the constraint.

In the case of the cay transform, the use of the configuration uptdate Eq. 18 and the closed form Eq. 21 yields

$$\mathbf{d}_{\mathbf{i}n+1}-\mathbf{d}_{\mathbf{i}n}=\theta\wedge\mathbf{d}_{\mathbf{i}_{n+\frac{1}{2}}} \quad (23)$$

Interpreting $\theta$ as the rotational increment, the following mid-point aproximation is taken

$$\theta=\Delta t\frac{\mathbf{w}_{n+1}+\mathbf{Q}_n^{n+1}\mathbf{w}_n}{2} \quad (24)$$

Now substituting Eq. 24 into Eq. 23 the following rotational velocity update formulae is obtained

$$\dot{\mathbf{d}}_{\mathbf{i}n+1}=\left[\mathbf{1}+cay[\theta]^T\right]^{-1}\times$$
$$\left[\frac{4}{\Delta t}(\mathbf{d}_{\mathbf{i}n+1}-\mathbf{d}_{\mathbf{i}n})-(\mathbf{1}-cay[\theta])\,\dot{\mathbf{d}}_{\mathbf{i}n}\right] \quad (25)$$

**Remark:** The inverse matrix in the above expression will not exist only for values of $\theta$ multiples of $2\pi$, which seems not to be a serious problem in practical computations.

### *3.2 Conservation of Angular Momentum*

In the present section, the conservation of angular momentum using the discrete form Eq. 16 and the update formulae Eq. 17 - Eq. 18 is shown.

**Proposition 3.1** *Assuming that there are not external loads (* $\mathbf{f}=\mathbf{0}$ *and* $\mathbf{f_i}=\mathbf{0}$*) the numerical algorithm based on Eq. 16, Eq. 17 and Eq. 18 conserves the angular momentum.*

**Proof:** Choose $\mathbf{p} = \mathbf{U} \wedge \mathbf{r}_{n+\frac{1}{2}}$, $\mathbf{g}_{\mathbf{i}n} = \mathbf{U} \wedge \mathbf{d}_{\mathbf{i}n}$ and $\mathbf{g}_{\mathbf{i}n+1} = \mathbf{U} \wedge \mathbf{d}_{\mathbf{i}n+1}$ for an arbitrary constant vector $\mathbf{U} \in R^3$. Inserting those quantities in Eq. 16 yields

$$\rho(\mathbf{v}_{n+1} - \mathbf{v}_n) \cdot \mathbf{r}_{n+\frac{1}{2}} + \sum_{i=1,3} I_i \{ \dot{\mathbf{d}}_{\mathbf{i}n+1} \cdot (\mathbf{U} \wedge \mathbf{d}_{\mathbf{i}n+1}) - \dot{\mathbf{d}}_{\mathbf{i}n} \cdot (\mathbf{U} \wedge \mathbf{d}_{\mathbf{i}n}) \} = \mathbf{0} \tag{26}$$

After some algebraic manipulation and exploring the properties of the vector product the above expression is reduced to

$$\mathbf{U} \cdot \{ \rho(\mathbf{r}_{n+1} \wedge \mathbf{v}_{n+1} - \mathbf{r}_n \wedge \mathbf{v}_n) + \sum_{i=1,3} I_i (\mathbf{d}_{\mathbf{i}n+1} \wedge \dot{\mathbf{d}}_{\mathbf{i}n+1} - \mathbf{d}_{\mathbf{i}n} \wedge \dot{\mathbf{d}}_{\mathbf{i}n}) \} = \mathbf{0} \tag{27}$$

in which the definition of angular momentum can be recognized, yielding

$$\mathbf{U} \cdot (\mathbf{J}_{n+1} - \mathbf{J}_n) = 0 \quad , \forall\, \mathbf{U} \in R^3 \tag{28}$$

which implies the conservation of angular momentum. It is worthwhile to remark that the conservation of angular momentum does not depend on the choice of exponential map or cay transform.

### *3.3 Conservation of Energy*

This section is devoted to the proof of the conservation of energy assured by the use of the proposed algorithm when the cay transform is used, which is summarised in the following propositon

**Proposition 3.2** *Assuming that the external loads, $f$ and $f_i$, are dead loads, the numerical algorithm based on Eq. 16, Eq. 17 and Eq. 18 conserves energy.*

**Proof:** Choose $\mathbf{p} = \mathbf{r}_{n+1} - \mathbf{r}_n$, $\mathbf{g}_{\mathbf{i}n} = \theta \wedge \mathbf{d}_{\mathbf{i}n}$ and $\mathbf{g}_{\mathbf{i}n+1} = \theta \wedge \mathbf{d}_{\mathbf{i}n+1}$ for $\theta$ defined in in Eq. 20. Inserting those quantities in Eq. 16 and introducing the orthogonal transformations $Q_0^n$ and $Q_0^{n+1}$ between the initial configuration and those in, respectively, $t_n$ and $t_{n+1}$ yields

$$\rho(\mathbf{v}_{n+1} - \mathbf{v}_n) \cdot (\mathbf{r}_{n+1} - \mathbf{r}_n) + \sum_{i=1}^{3} I_i \{ Q_0^{n+1T} \dot{\mathbf{d}}^{\,i}_{\mathbf{I}n+1} \cdot Q_0^{n+1T} (\theta \wedge \mathbf{d}_{\mathbf{i}n+1}) - Q_0^{nT} \dot{\mathbf{d}}_{\mathbf{I}n} \cdot Q_0^{nT} (\theta \wedge \mathbf{d}_{\mathbf{i}n}) \} = \mathbf{f}_{n+\frac{1}{2}} \cdot (\mathbf{r}_{n+1} - \mathbf{r}_n) - \sum_{i=1}^{3} \mathbf{f}_{\mathbf{i}n+\frac{1}{2}} \cdot \theta \wedge \mathbf{d}_{\mathbf{i}n+\frac{1}{2}} \tag{29}$$

After a direct manipulation, introducing the convective representations, see Simo and Tarnow(1995), $\boldsymbol{\Theta} = Q_0^{nT} \theta$ and $\mathbf{V}_{\mathbf{i}n} = Q_0^{nT} \dot{\mathbf{d}}_{\mathbf{i}n}$ and using that $Q_0^{nT} (\theta \wedge \mathbf{d}_{\mathbf{i}n}) = \boldsymbol{\Theta} \wedge \mathbf{D}_{\mathbf{i}}$, the equation Eq. 29 results in

$$\rho(\mathbf{v}_{n+1} - \mathbf{v}_n) \cdot (\mathbf{r}_{n+1} - \mathbf{r}_n) + \sum_{i=1}^{3} I_i \{ \mathbf{V}_{\mathbf{i}n+1} \cdot (\boldsymbol{\Theta} \wedge \mathbf{d}_{\mathbf{i}n+1}) - \mathbf{V}_{\mathbf{i}n} \cdot (\boldsymbol{\Theta} \wedge \mathbf{d}_{\mathbf{i}n}) \} = \mathbf{f}_{n+\frac{1}{2}} \cdot (\mathbf{r}_{n+1} - \mathbf{r}_n) - \sum_{i=1}^{3} \mathbf{f}_{\mathbf{i}n+\frac{1}{2}} \cdot \theta \wedge \mathbf{d}_{\mathbf{i}n+\frac{1}{2}} \tag{30}$$

Now introducing in Eq. 30 the convective version of the update formulae Eq. 24, Eq. 17 and Eq. 23 yields

$$\Delta t \{ \rho (\frac{\mathbf{v}_{n+1}^2}{2} - \frac{\mathbf{v}_n^2}{2}) + \sum_{i=1}^{3} \frac{I_i}{2} (\mathbf{V}_{\mathbf{i}n+1}^2 - \mathbf{V}_{\mathbf{i}n}^2) \} = \mathbf{f}_{n+1} \cdot \mathbf{r}_{n+1} - \mathbf{f}_n \cdot \mathbf{r}_n + \sum_{i=1}^{3} \mathbf{f}_{\mathbf{i}n+1} \cdot \mathbf{d}_{\mathbf{i}n+1} - \mathbf{f}_{\mathbf{i}n} \cdot \mathbf{d}_{\mathbf{i}n} \tag{31}$$

Defining the total energy as $\boldsymbol{H} = T + V$ the above relation leads to

$$\boldsymbol{H}_{n+1} - \boldsymbol{H}_n = 0 \tag{32}$$

which implies in the conservation of the energy.

**Remark:** Indeed, the conservation of energy when using the exponential map is also achieved if $\mathbf{f}_{\mathbf{i}} = \mathbf{0}$.

## 4 Numerical Algorithm

In the present chapter the numerical scheme is presented. The discrete equations introduced in the last chapter, namely Eq. 16, Eq. 17 and Eq. 18, result in a nonlinear constrained problem, which will be solved by means of a Newton technique. From the mathematical point of view, the rotational and translational motions are not coupled and, thus, might be solved independently. The main steps concerning the rotational components are shown below. The translational problem is linear and is solved by a conventional procedure, which will be not detailed here.

Assume that at $t_n$ the following initial data are known :

$$(\mathbf{d}_{\mathbf{i}n}, \dot{\mathbf{d}}_{\mathbf{i}n}) \in K \times dK$$

The objective is to obtain an approximation

$$(\mathbf{d}_{\mathbf{i}n+1}, \dot{\mathbf{d}}_{\mathbf{i}n+1}, \lambda_{ij_{n+\frac{1}{2}}}) \in K \times dK \times R^9$$

to the actual solution $(\mathbf{d}_{\mathbf{i}}(t_n), \dot{\mathbf{d}}_{\mathbf{i}}(t_{n+1}), \lambda_{ij}(t_n + \frac{\Delta t}{2}))$. The main steps of the algorithm are summarised below

**Step 0.** Initialization for time step in $[t_n, t_{n+1}]$. Define a predictor for directors and velocities:

$$\mathbf{d}^{\mathbf{0}}_{\mathbf{i}\,n+1} = \mathbf{d}_{\mathbf{i}n} \quad ; \quad \dot{\mathbf{d}}^{\mathbf{0}}_{\mathbf{i}\,n+1} = -\dot{\mathbf{d}}_{\mathbf{i}n}$$

Newton Loop: For k=0,1,2,...

**Step 1.** Check for Convergence: Compute the vector

$$\begin{aligned}\mathbf{R}^k_{n+1} &= I_1(\dot{\mathbf{d}}^k_{\mathbf{1}n+1}\cdot\mathbf{g}_{\mathbf{1}n+1} - \dot{\mathbf{d}}_{\mathbf{1}n}\cdot\mathbf{g}_{\mathbf{1}n}) + \\ &I_2\{\dot{\mathbf{d}}^k_{\mathbf{2}n+1}\cdot\mathbf{g}_{\mathbf{2}n+1} - \dot{\mathbf{d}}_{\mathbf{2}n}\cdot\mathbf{g}_{\mathbf{2}n}) + \\ &I_3\{\dot{\mathbf{d}}^k_{\mathbf{3}n+1}\cdot\mathbf{g}_{\mathbf{3}n+1} - \dot{\mathbf{d}}_{\mathbf{3}n}\cdot\mathbf{g}_{\mathbf{3}n}\} \\ &+\Delta t\{\sum_{i=1}^{3}\mathbf{f}_{\mathbf{i}n+\frac{1}{2}}\cdot\mathbf{g}_{\mathbf{i}n+\frac{1}{2}}\}\end{aligned} \tag{33}$$

Vector $\mathbf{R}^k_{n+1}$ has nine components, each one associated to a specific choice of $\mathbf{g_i}$ (e.g.: $\mathbf{g_i}=\mathbf{d_j}$ for $i,j=1,3$ with $\mathbf{g_k}=\mathbf{0}$ *and* $\mathbf{g_l}=\mathbf{0}$ for $k,l\neq i$).

Compute the lagrange multipliers $\lambda_{ij}{}^k_{n+\frac{1}{2}}$ through vector $\mathbf{R}^k_{n+1}$ calculated above. Each lagrange multiplier will be computed in order to have the equation Eq. 16 satisfied for the specific choice of $\mathbf{g_i}$ introduced above. Thus, for instance, $\lambda_{11}{}^k_{n+\frac{1}{2}} = 0.5R(1)^k_{n+1}$, where $R(1)$ denotes for the first component of $\mathbf{R}^k_{n+1}$.

Compute the residual vector $\mathbf{b}^k_{n+1}$ by substituting the values of $\mathbf{d_i}^k_{n+1}$ in Eq. 16 and choosing $\mathbf{g_i}=U\wedge\mathbf{d_i}$, which represents that $\mathbf{g_i}\in dK$, considering $\mathbf{b}(i)$ associated to $U=\mathbf{d_i}$.

IF $||\mathbf{b}^k_{n+1}||\leq$ tolerance then begin a new time step ($n+1\rightarrow n$ ; go to Step 0). ELSE continue

**Step 2.** Obtain the rotational increment $\hat{U}$

Compute the tangent matrix $K^k_{n+1}$ from the linearised form presented in Appendix B for $\mathbf{g_i}=U\wedge\mathbf{d_i}$ and $\hat{\mathbf{g}}_\mathbf{i}=\hat{\mathbf{U}}\wedge\mathbf{d_i}$

Computation of $\hat{\mathbf{U}}$ solving the linear system

$$K^k_{n+1}\hat{\mathbf{U}} = R^k_{n+1}$$

**Step 3.** Update the configuration and the velocity for a given rotational increment $\hat{U}$ by using formulae Eq. 18 with Eq. 19 (or Eq. 21) and Eq. 22 (or Eq. 25) with

$[\mathbf{Q}^{n+1}_n]^{k+1} = \exp(\hat{U})\mathbf{Q}^{n+1}_n]^k$

or

$[\mathbf{Q}^{n+1}_n]^{k+1} = cay(\hat{U})\mathbf{Q}^{n+1}_n]^k$

**Remark:** From the predictor choice $[\mathbf{Q}^{n+1}_n]^0=\mathbf{1}$

**Step 4.** Begin a new iteration; $k+1\rightarrow k$; go to Step 2

## 5 Numerical Simulations

In this section, two representative numerical simulations are presented in order to illustrate the performance of the proposed algorithm. Both situations, which are also examined by Simo and Wong(1991) and Park and Chiou(1993), are chosen due to the presence of conserved quantities during the motion. In fact, the reproduction of this conservation behavior by the numerical algorithm is considered a demonstration of stability and accuracy. The key idea is to treat problems in which the reliability of the proposed numerical modelling can be assessed even for the long-time dynamics.

In the first simulation, it is considered the motion of a symmetrical top with total mass $M$ in a uniform gravitational field $-g\ \mathbf{e_3}$. The vector $\mathbf{e_3}$ belongs to an inertial frame $\{\mathbf{e_i}\}$. The same numerical values of Simo and Wong (1991) were adopted: $Mg=20, l=1, I_{11}=I_{22}=5.$ and $I_{33}=1$. The parameter $l$ denotes the distance between the bottom of the top and its center of gravity. The following initial conditions are also adopted:

$$\mathbf{w}(0)=50\,\mathbf{d_3}(0); \qquad \mathbf{d_i}(0)=\exp\,(0.3\mathbf{e_i})$$

Figs. 1–4 shows the numerical results obtained for time step $\Delta t=0.001$. The total energy remains constant during the observed period as well as the component of the spatial angular momentum in the direction $\mathbf{e_3}$,$h_3$. Both facts demonstrate the stability and accuracy of the proposed formulation in the present example as this conservation behaviour is to be expected. Fig. 4 presents the nutation and precession of the top about its fixed contact point. For the present example [Simo and Wong(1991)] one has the following relations for the angular frequencies of nutation $w_n$ and precession $w_p$:

$$w_n=\frac{I_{33}}{I_{11}}(\mathbf{w}\cdot\mathbf{d_3}) \quad and \quad w_p=\frac{Mgl}{I_{33}(\mathbf{w}\cdot\mathbf{d_3})}$$

For the chosen numerical parameters these relations lead to values $w_n=10.0$ and $w_p=0.4$. In the present numerical simulation $w_n=9.9999$ and $w_p=0.4000$ were obtained.

The numerical solution obtained with $\Delta t=0.001$ will be considered a good approximation to the true solution, which is not known, in order to assess the main features of the proposed numerical scheme. In Figs. 5, 6 and 7 the numerical solution using $\Delta t=0.04$ (40 times the first one) is depicted. A constant oscillation is exhibited by the total energy, although it does not represent a sign of numerical instability as it is too small and constant in the long period of observation. Indeed, the conservation of energy is achieved using the cay transform, which is presented in Fig. 8.

It is also important to observe the preservation of the component $h_3$ of the Spatial Angular Momentum. The values obtained for the angular velocities of nutation and precession are, respectively, $w_n=9.5460$ and $w_p=0.4190$.

In order to stress the importance of conservation algorithms in the simulation of the long term dynamics, the present situation is analysed using the proposed numerical method and another one which is an extension to nonlinear situations of the Newmark algorithm. This extension is also used, for comparison purposes, by Simo and Wong(1994). All the values are the same of the above situation, except the initial angular velocity and the inertia moments, which are given by:

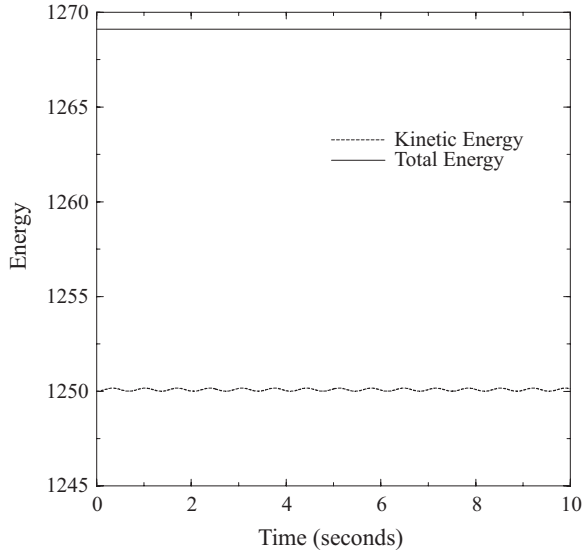


**Figure 1** : Kinetic and Total Energy

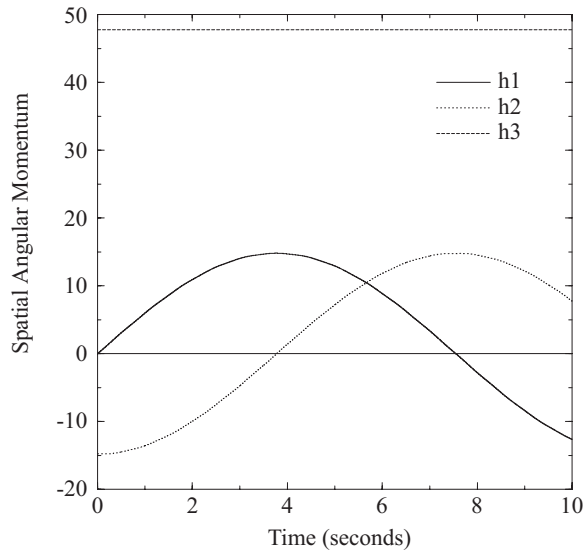


**Figure 2** : Spatial Angular Momentum

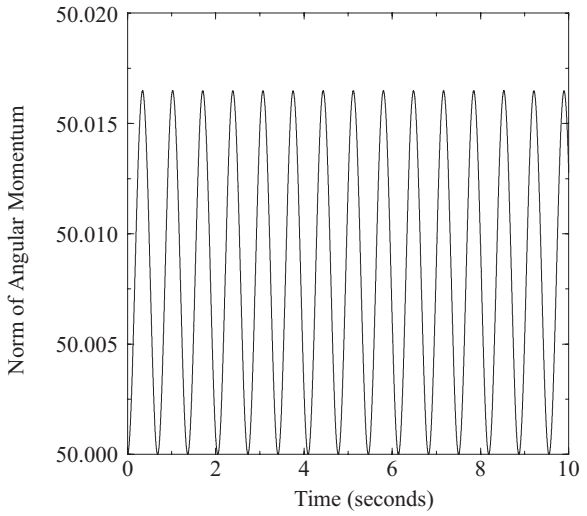


**Figure 3** : Norm of Angular Momentum

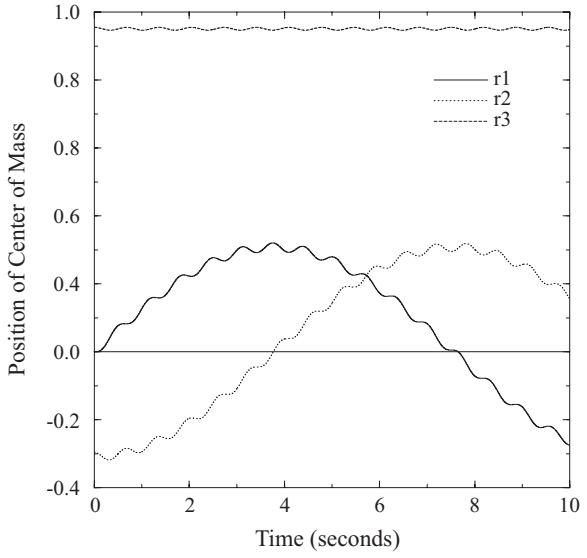


**Figure 4** : Position of Center of Mass

$\mathbf{w}(0) = 8\mathbf{d_1}(0) + 15\mathbf{d_2}(0) + 4\mathbf{d_3}(0)$ and $I_{11} = 1.0$, $I_{22} = 2.2$ and $I_{33} = 3$.

In Figs. 8 and 9 the quantities to be conserved, namely the total energy and the component of the angular momentum in the $\mathbf{e_3}$ direction, computed with the two algorithms are depicted. The adapted Newmark algorithm corresponds to the mid-point rule, which conserves energy in the linear range. As it is presented in figures below, this algorithm presents an expressive variation of those quantities, leading to a not reliable solution. The proposed conserving algorithm shows, once again, its capability of reproducing the conservation characteristics which represents a stable behavior and the capture of key aspects of the long term dynamics. In the present simulation a time step of 0.06 was adopted.

The second numerical experiment deals with the unstable rotational motion about the intermediate moment of inertia of a rigid body. This simulation is performed according to the three following load steps: (i) At time $t = 0$ a constant torque is applied to the body at rest in the direction coincident with the intermediate moment of inertia; (ii) At time $t = t^*$, the torque is removed and another one is applied to the body for a short duration equal to the time step $\Delta t$ ; (iii) Finally, the rigid body undergoes a torque free motion. The situation is summarized in the torque history given below:

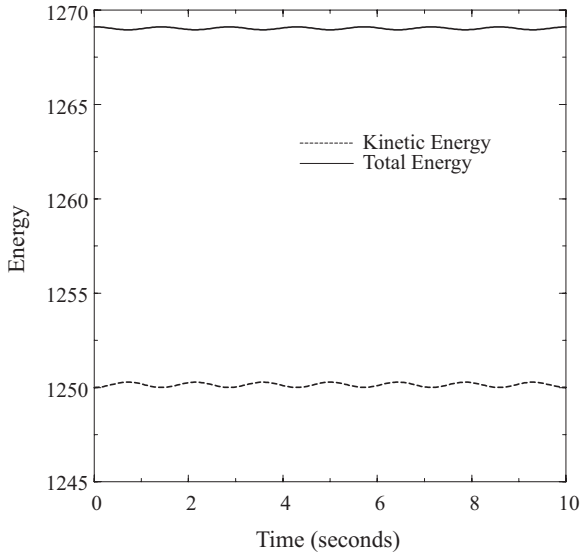


**Figure 5** : Kinetic and Total Energy ($\Delta t = 0.04$)

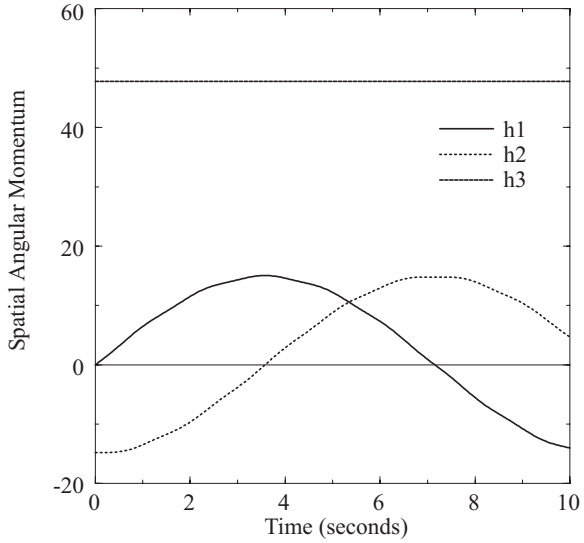


**Figure 6** : Spatial Angular Moment($\Delta t = 0.04$)

$$\mathbf{m} = \begin{cases} A_1\mathbf{e_1} & 0 \le t \le t^* \\ A_2\mathbf{e_2} & t^* \le t \le t^* + \Delta t \\ 0 & t > t^* + \Delta t \end{cases}$$

where $A_1$ and $A_2$ are constants given by: $A_1 = 20.$ and $A_2 = \frac{0.2}{\Delta t}$. The others parameters used in the simulations are: $t^* = 2.0 - \Delta t$, $I_{11} = 5$, $I_{22} = 10$ and $I_{33} = 1$. Although those inertia moments do not correspond to a real rigid body, as the sum of two of them, namely: $I_{11}$ and $I_{33}$, is not greater than the third one, they were taken to make comparisons with the results presented in Simo and Wong(1991) and Park and Chiou(1993).

The body begins at rest, thus the initial velocities are zero. As the resultant force acting on the body is zero during the motion, the center of mass stays at rest. Hence, this is a pure rotational

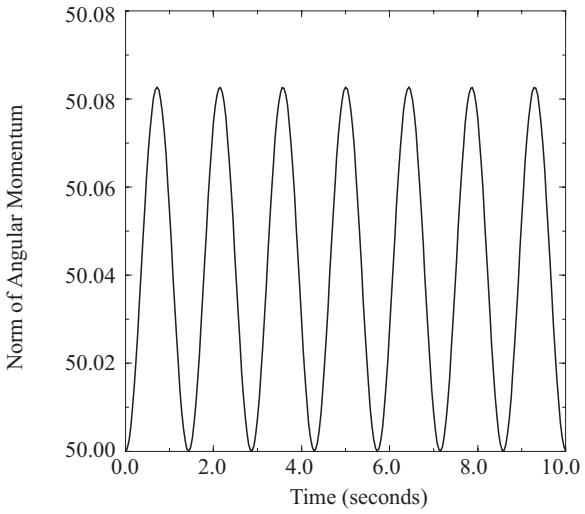


**Figure 7** : Norm of Angular Momentum($\Delta t = 0.04$)

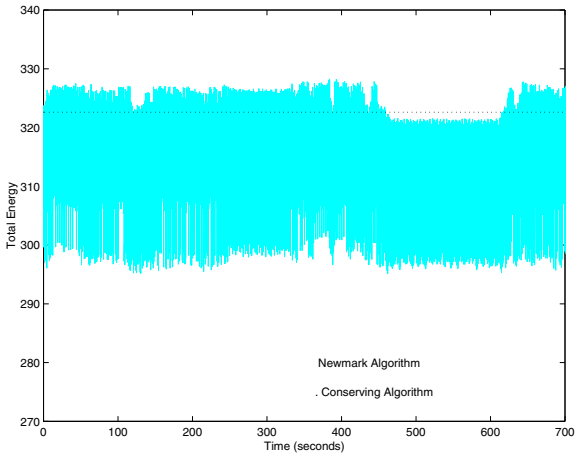


**Figure 8** : Total Energy

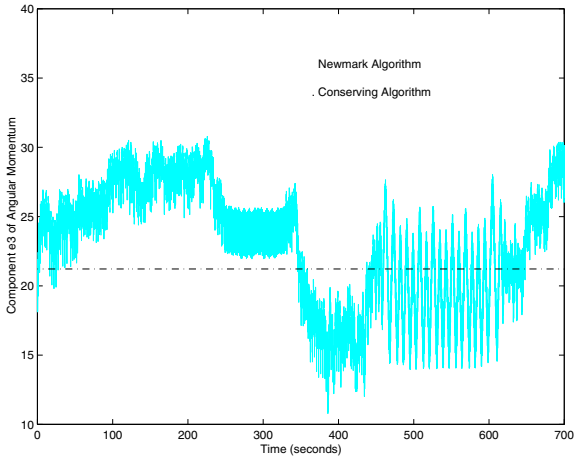


**Figure 9** : Angular Momentum

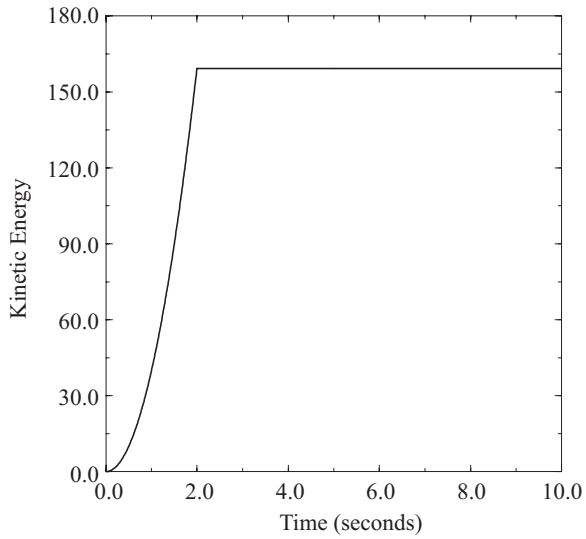


**Figure 10** : Kinetic Energy

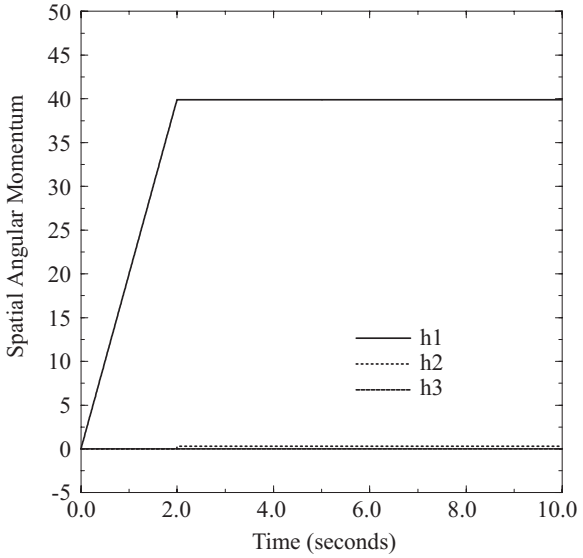


**Figure 12** : Spatial Angular Momentum

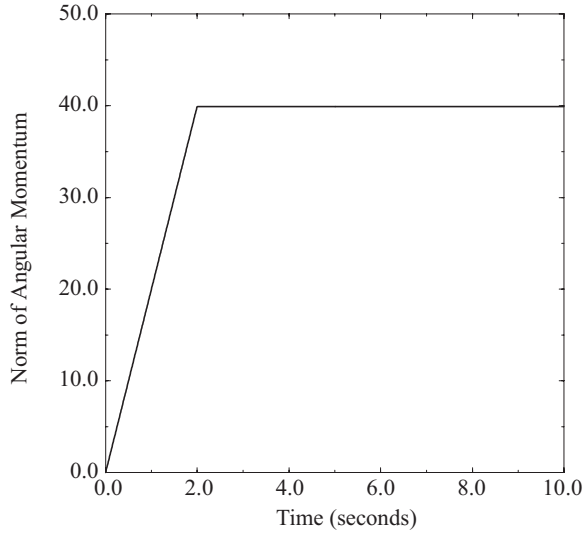


**Figure 11** : Norm of Angular Momentum

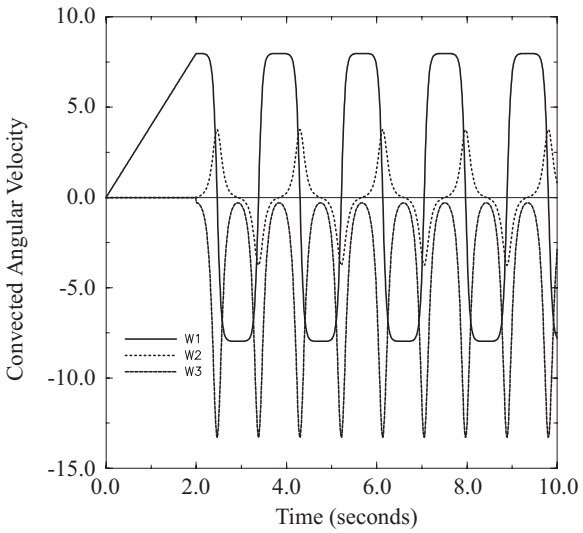


**Figure 13** : Convected Angular Velocity

situation in which the angular momentum and the total energy are conserved after the instant $t^* + \Delta t$.

Two distinct time-steps were chosen for the numerical experiments, namely: 0.1 and 0.01. The solution obtained using the second time step will be taken as a reference and it is summarized in Figs. 10 –13. The first three, kinetic energy, norm of angular momentum and spatial angular momentum, demonstrate the good conservation capabilities of the proposed algorithm. In the last one, Fig. 13, the convected angular velocity is shown.

The results obtained using the $\Delta t = 0.1$ are presented in Figs. 14 – 17. In the present modelling, although the applied moment introduced above remains constant during the intervals $[0, t^*]$ and $[t^*, t^* + \Delta t]$, for this case the applied load depends on the assumed configuration due to the definition Eq. 13. This fact explains the discrepancy observed between the results using the two different time steps. Indeed, $\Delta t = 0.1$ implies in rather large values of incremental rotations and leads to inaccurate results. Nevertheless, the energy and angular momentum are still conserved.

## 6 Concluding Remarks

A variational formulation to the rigid body problem was presented in order to provide a robust formulation, which not only afford a general unified approach, but also is very convenient

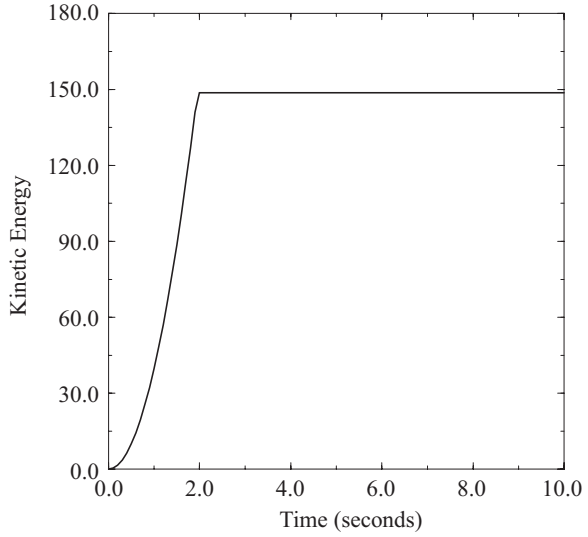


**Figure 14** : Kinetic Energy

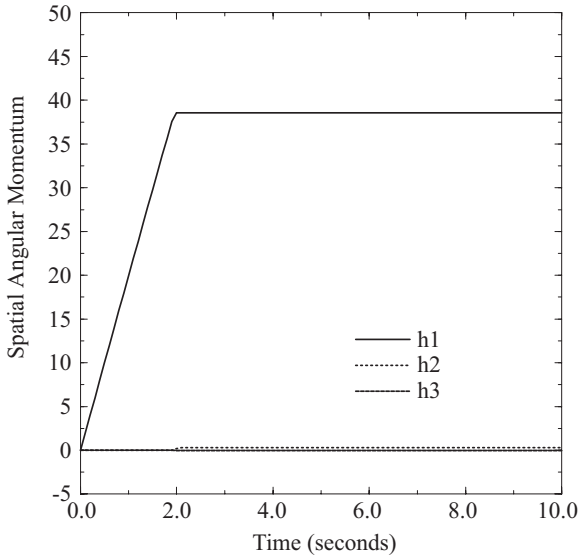


**Figure 16** : Spatial Angular Momentum

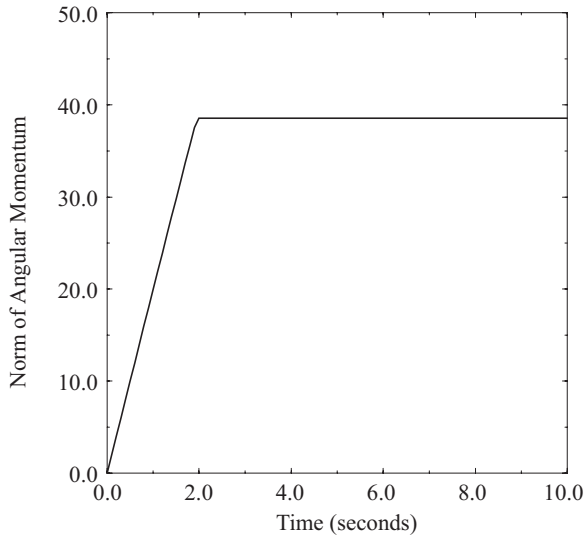


**Figure 15** : Norm of Angular Momentum

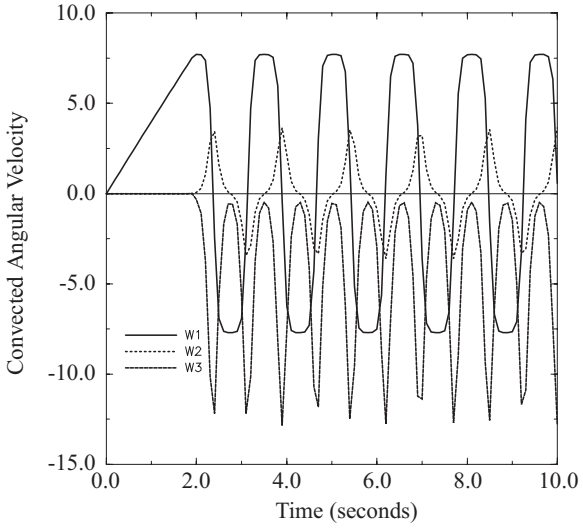


**Figure 17** : Convected Angular Velocity

from the numerical standpoint.

The main question in dealing with large rotations is circumvented by the use of lagrange multipliers, which will imply the augmentation of the number of degrees of freedom. By the way, this can be avoided in numerical applications using a similar scheme to that used in Rochinha(1990) and Le Tallec, Mani and Rochinha(1992), where the lagrange multipliers are computed with little computational effort.

Finally, a similar approach can be used in the case of flexible links like rods. A first attempt is presented in Campos(1996). So, the present framework seems to be very convenient to be used in the modelling of flexible multibody systems.

## 7 References

**Antman, S.S; Kenney, C.S.**(1981): "Large buckled states of nonlinear elastic rods under torsion, thrust and gravity", *Arch. Rat. Mech. Anal.* 76, 289–337.

**Bailey, C.D.** (1987): "Dynamics and the calculus of variations". *Computer Methods in Applied Mechanics and Engineering* 60, 275–287.

**Balysis, A.; Isaacson, E.**(1975): "How to make your algorithm conservative". *American Mathematical Society*, A594–A595.

**Bauchau, O.A.; Damilano, G. ; Theron, N.J.** (1995): "Nu-

merical integration of nonlinear elastic multi-body systems". *International Journal for Numerical Methods in Engineering* 38, 2727–2751.

**Borri, M.; Mello, F. ;Atluri, S.N.**(1991): "Variational approaches for dynamics and time–finite elements: Numerical studies", *Computational Mechanics* 7, 49–76.

**Campos, A.D. ;Rochinha, F.A**(1996): "Dynamics of Rods: Numerical Formulation ", *Proceedings of Advances in Computational Technique for Structural Engineering*,Budapest,Hungary, 239–246.

**Cardona, A.; Géradin, M .** (1989): "Time integration of the equations of motion in mechanism analysis", *Computers & Structures* 33, 801–820.

**Crisfield, M.A.; Shi, J.** (1994): "A co-rotational element/time-integration strategy for non-linear dynamics". *International Journal for Numerical Methods in Engineering* 37, 1897–1913.

**Downer, J.D.; Park, K.C.; Chiou,E.** (1992): "Dynamics of flexible beams for multibody systems: A computational procedure", *Comp. Meth. Appl. Mech. and Engng.* 96, 373–408.

**Galvanetto, U.; Crisfield, M.A.** (1996): "An energy-conserving co-rotational procedure for the dynamics of planar beam structures". *International Journal for Numerical Methods in Engineering* 39, 2265–2282.

**Géradin, M.; Rixen, D.** (1995): "Parametrization of finite rotations in computational dynamics: a review". *Revue Européene des Éléments Finis* 4, 497–553.

**Gonzalez, O.** (1996): *"Design and Analysis of Conserving Integrators for Nonlinear Hamiltonian Systems With Symmetry"* . Stanford University, Department of Mechanical Engineering, PhD Thesis.

**Hughes, P.C.** (1986): "Spacecraft Attitude Dynamics", Wiley, New York.

**Hughes, T.J.R.; Liu, W.K.; Caughy, P.** (1978): "Transient finite element formulations that preserve energy".*J.Appl. Mech. ASME* 45, 366–370.

**Iura,M., Atluri, S.N.** (1995): " Dymamica Analysis of Planar Flexible Beams with finite Rotations by using Inertial and Rotating Frames ", *Computer & Structures* 55 (3), pp.453-462.

**Kolmanovsky, I. ; McClamroch, N.H.**(1995): " Developments in Nonholonomic Control Problems ", *IEEE Control Systems Journal* 15, 20 – 36.

**LaBudde, R.A.; Greenspan, D.** (1976a): "Energy and Momentum Conserving Methods of Arbitrary Order for the numerical integration of equations of motion. Part I". *Numerisch Mathematik* 25, 323–346.

**LaBudde, R.A.; Greenspan, D.** (1976b): "Energy and Momentum Conserving Methods of Arbitrary Order for the numerical integration of equations of motion. Part II". *Numerisch Mathematik* 26, 1–16.

**Le Tallec, P.; Mani, S.A.; Rochinha, F.A.**( 1992): "Finite element computation of hyperelastic rods in large displacements", *RAIRO – Math. Model. Num. Anal.* 26, 325–346.

**Lewis, D. ; Simo, J.C.** (1994): "Conserving algorithms for the Dynamics of Hamiltonian Systems on Lie Groups".*J. Nonlinear Sci.* 4,253–299.

**Meirovitch, L.** (1970): *"Methods of Analytical Dynamics"*, McGraw-Hill, New York.

**Quadrelli, M.B.; Atluri, S.N.**(1999) : " Mixed Variational Principles in Space and Time for Elastodynamics Analysis ", *ACTA MECH* 136,pp.193-208 .

**Richtmyer R.D.; Morton, K.W.** (1967): *"Difference methods for initial value problems"*, 2nd edn., Interscience, New York.

**Rochinha, F.A.**(1990): *"Modelling and numerical simulation of rods "*,(in portuguese), PhD Thesis, PUC–Rio, Rio de Janeiro, Brazil.

**Sharf, I.**(1996): " Geometrically Non-Linear Beam Element for Dynamics Simulation of Multibody Systems ", *Int. J. Num. Meth. Engng.* 39, pp. 763 – 786.

**Simo, J.C.; Wong, K.K.**( 1991): "Unconditionally stable algorithms for rigid body dynamics that exactly preserve energy and momentum", *Int. J. Numer. Methods Eng.* 31, 19–52.

**Simo, J.C.; Tarnow, N. ; Wong, K.** (1992): "Exact energy-momentum conserving algorithms and sympletic schemes for nonlinear dynamics". *Computer Methods in Applied Mechanics and Engineering* 100, 63–116.

**Simo, J.C.;Gonzalez, O.** (1993): "Assessment of energy-momentum and symplectic schemes for stiff dynamical systems". American Society of Mechanical Engineers, ASME Winter Annual Meeting, New Orleans, Louisiana.

**Simo, J.C.; Tarnow, N.** (1995): "Non-linear dynamics of three-dimensional rods: exact energy and momentum conserving algorithms". *International Journal for Numerical Methods in Engineering* 38, 1431–1473.

**Trindade, M. A.; Sampaio, R.** (1999): "Finite rotations parametrisations: a review", (in portuguese), to appear in *RBCM - J. of the Braz.Soc. Mechanical Sciences*, avaailable in http://www.mec.puc-rio.br/prof/rsampaio/rsampaio.html

**Whittaker, E.T.** (1944): *"A treatise on analytical dynamics"*. Dover Publications, New York.

**Vu-Quoc, L.; Simo, J.C.**( 1988): "Dynamics of earth-orbiting flexible satellites with multibody components", *J.Guidance and Control* 1, 549–558.

**Zhong, G.; Marsden, J.E.** (1988): "Lie-Poisson Hamilton-Jacobi theory and Lie-Poisson Integrators". *Physics Letters A* 3, 134–139.

## Appendix A: Equivalence Between the Variational Formulation and Classical Euler Equations for a Rigid Body

In the present appendix the equivalence between the variational formulation Eq. 15 and the Euler equations for the rigid body dynamics is shown.

For the sake of completeness, the Euler equations are reviewed below:

- Translational Motion

$$M\dot{\mathbf{v}} = \mathbf{f} \tag{34}$$

$$\dot{\mathbf{r}} = \mathbf{v} \tag{35}$$

- Rotational Motion

$$\mathbf{I}\dot{\mathbf{w}} = \mathbf{m} \tag{36}$$

$$\dot{\mathbf{Q}} = \hat{\mathbf{w}}\mathbf{Q} \tag{37}$$

The first equations are obtained from the variational formulation Eq. 15 by choosing $\mathbf{g_i} = \mathbf{0}$ and performing an integration by parts in the others terms yielding

$$\int_{t1}^{t2} \{m\dot{\mathbf{v}} \cdot \mathbf{p} - \mathbf{f} \cdot \mathbf{p}\} dt = \mathbf{0} \quad \forall\, \mathbf{p} \in R^3 \tag{38}$$

which implies directly the first equation of Eq. 35. The second equation of Eq. 35 is just the definition of the translational velocity which is also used in the variational formulation.

The second step in the proof consists in obtaining the equivalence of the Eq. 37 and Eq. 15. Remembering that $\mathbf{Q} = \mathbf{d_i} \otimes \mathbf{D_i}$ and thus $\dot{\mathbf{Q}} = \dot{\mathbf{d}}_\mathbf{i} \otimes \mathbf{D_i}$ and the relation between the angular velocity and the director velocity yields

$$\dot{\mathbf{Q}} = (\hat{\mathbf{w}}\mathbf{d_i}) \otimes \mathbf{D_i} \tag{39}$$

which, with the use of a tensorial product property, implies the equivalence with the second equation of Eq. 37.

Now, performing an integration by parts in (15) , introducing $\mathbf{p} = \mathbf{0}$ and $\mathbf{g_i} = U \wedge \mathbf{d_i}$ and rearranging terms the following expression is obtained

$$\sum_{i=1}^{3} I_i(\mathbf{d_i} \wedge \ddot{\mathbf{d}}_\mathbf{i}) - \sum_{i=1}^{3} \mathbf{d_i} \wedge \mathbf{f_i}\} dt] = \mathbf{0}, \qquad \forall U \in R^3 \tag{40}$$

In Eq. 40 the coincidence between the directors and the principal directions of inertia is assumed. Now, substituting the relation $\mathbf{d_i} \wedge \ddot{\mathbf{d}}_\mathbf{i}$ and Eq. 5 in Eq. 40 and combining terms yields

$$U \cdot [\int_{t1}^{t2} \{\mathbf{I}\boldsymbol{\alpha} + \mathbf{w} \wedge (\mathbf{I}\mathbf{w}) + \mathbf{m}\} dt] = 0, \qquad \forall U \in R^3 \tag{41}$$

Thus, finally, using standard arguments of the calculus of variations and recognizing in the two first terms of the integral the time derivative of $\mathbf{Iw}$, the first equation of Eq. 37 (balance of angular momentum ) is obtained.

## Appendix B: Exact Linearization of the Discrete Equations

As the numerical algorithm introduced in section 4 is based on a Newton techinique, one needs to have a linearized version of Eq. 16, Eq. 17 and Eq. 18 around $(\mathbf{r}_{n+1}, \mathbf{d_i}_{n+1}, \lambda_{ij_{n+\frac{1}{2}}}, \dot{\mathbf{r}}_{n+1}, \dot{\mathbf{d}}_{\mathbf{i}n+1})$. This linearization of the discrete balance equation Eq. 16 is presented below

$$\begin{aligned}
&\rho\left(\frac{\partial \mathbf{v}_{n+1}}{\partial \mathbf{r}_{n+1}}\hat{\mathbf{p}}\right) \cdot \mathbf{p} + \sum_{j=1}^{3} I_1 \left(\frac{\partial \dot{\mathbf{d}}_{\mathbf{1}n+1}}{\partial \mathbf{d_j}_{n+1}}\hat{\mathbf{g}}_{\mathbf{j}_{n+1}}\right) \cdot \mathbf{g_1}_{n+1} + \\
&I_2\left(\frac{\partial \dot{\mathbf{d}}_{\mathbf{2}n+1}}{\partial \mathbf{d_j}_{n+1}}\hat{\mathbf{g}}_{\mathbf{j}_{n+1}}\right) \cdot \mathbf{g_2}_{n+1} + I_3\left(\frac{\partial \dot{\mathbf{d}}_{\mathbf{3}n+1}}{\partial \mathbf{d_j}_{n+1}}\hat{\mathbf{g}}_{\mathbf{j}_{n+1}}\right) \cdot \mathbf{g_3}_{n+1} \\
&+ \frac{1}{2}\Delta t \sum_{i,j=1}^{3} \hat{\lambda_{ij}}_{n+\frac{1}{2}}(\mathbf{d_i}_{n+1} \cdot \mathbf{g_j}_{n+1} + \mathbf{d_j}_{n+1} \cdot \mathbf{g_i}_{n+1}) + \\
&\lambda_{ij_{n+\frac{1}{2}}}(\hat{\mathbf{g}}_{\mathbf{i}n+1} \cdot \mathbf{g_j}_{n+1} + \hat{\mathbf{g}}_{\mathbf{j}n+1} \cdot \mathbf{g_i}_{n+1}) = \\
&\Delta t\left(\left(\frac{\partial \mathbf{f}_{n+\frac{1}{2}}}{\partial \mathbf{r}_{n+1}}\right)\hat{\mathbf{p}} \cdot \mathbf{p} - \sum_{i=1}^{3}\sum_{j=1}^{3}\left(\frac{\partial \mathbf{f_i}_{n+\frac{1}{2}}}{\partial \mathbf{d_j}_{n+1}}\hat{\mathbf{g}}_{\mathbf{j}_{n+1}}\right) \cdot \mathbf{g_i}_{n+\frac{1}{2}}\right)
\end{aligned} \tag{42}$$

where $\hat{\mathbf{p}}$,$\hat{\mathbf{g}}_\mathbf{i}$ and $\hat{\lambda}$ are increments associated, respectively, to $\mathbf{r}$,$\mathbf{d_i}$ and $\lambda$

The partial derivatives of the velocities are obtained from uptdade formulae introduced in section 3, yielding

$$\frac{\partial \mathbf{v}}{\partial \mathbf{r}}\hat{\mathbf{p}} = \frac{\Delta t}{2}\hat{\mathbf{p}} \tag{43}$$

$$\frac{\partial \dot{\mathbf{d}}_\mathbf{i}}{\partial \mathbf{d_j}}\hat{\mathbf{g}}_\mathbf{j} = \delta_{ij}\frac{\Delta t}{2}\hat{\mathbf{g}}_\mathbf{j} - \left(1 - \delta_{ij}(\hat{\mathbf{g}}_\mathbf{j} \otimes \mathbf{d_j}_n)\right)\dot{\mathbf{d}}_{\mathbf{i}n} \tag{44}$$

whether the exponential map is used, or

$$\begin{aligned}
&\frac{\partial \dot{\mathbf{d}}_\mathbf{i}}{\partial \mathbf{d_j}}\hat{\mathbf{g}}_\mathbf{j} = [\mathbf{1} + cay[\theta]^T]^{-1} \\
&\left(4\frac{\delta_{ij}}{\Delta t}\hat{\mathbf{g}}_\mathbf{i} - (1 - \delta_{ij})(\hat{\mathbf{g}}_\mathbf{j} \otimes \mathbf{d_j}_n)\dot{\mathbf{d}}_{\mathbf{i}n} - (\mathbf{d_j}_n \otimes \hat{\mathbf{g}}_\mathbf{j})\dot{\mathbf{d}}_{\mathbf{i}n+1}\right)
\end{aligned} \tag{45}$$

when using the cay operator.